

Purdue University
Purdue e-Pubs

International Refrigeration and Air Conditioning
Conference

School of Mechanical Engineering

2016

An Experimental Investigation of Convective Boiling Heat Transfer Using Alternative and Natural Refrigerants Inside Horizontal Microchannels

Nguyen-Ba Chien

Chonnam National University, Korea, Republic of (South Korea), chienfm50@gmail.com

Pham-Quang Vu

Chonnam National University, Korea, Republic of (South Korea), vu@chonnam.ac.kr

Kwang-Il Choi

Chonnam National University, Korea, Republic of (South Korea), imcg@chonnam.ac.kr

Jong-Taek Oh

Chonnam National University, Korea, Republic of (South Korea), ohjt@chonnam.ac.kr

Follow this and additional works at: <http://docs.lib.purdue.edu/iracc>

Chien, Nguyen-Ba; Vu, Pham-Quang; Choi, Kwang-Il; and Oh, Jong-Taek, "An Experimental Investigation of Convective Boiling Heat Transfer Using Alternative and Natural Refrigerants Inside Horizontal Microchannels" (2016). *International Refrigeration and Air Conditioning Conference*. Paper 1669.
<http://docs.lib.purdue.edu/iracc/1669>

This document has been made available through Purdue e-Pubs, a service of the Purdue University Libraries. Please contact epubs@purdue.edu for additional information.

Complete proceedings may be acquired in print and on CD-ROM directly from the Ray W. Herrick Laboratories at <https://engineering.purdue.edu/Herrick/Events/orderlit.html>

An Experimental Investigation of Convective Boiling Heat Transfer Using Alternative and Natural Refrigerants inside Horizontal Microchannels

Nguyen-Ba Chien¹, Pham-Quang Vu¹, Kwang-Il Choi², Jong-Taek Oh^{2*}

¹Graduate School, Chonnam National University, San 96-1, Dunduk-Dong, Yeosu, Chonnam 59626, Republic of Korea

²Department of Refrigeration and Air Conditioning Engineering, Chonnam National University, San 96-1, Dunduk-Dong, Yeosu, Chonnam 59626, Republic of Korea

* Corresponding Author: Email: ohjt@chonnam.ac.kr, Tel: +82-61-659-7273; Fax: +82-61-659-7279

ABSTRACT

In present study, the two phase flow boiling heat transfer coefficient and pressure drop of R410A, R32 and R290 in microchannels are demonstrated. The experimental data were conducted in horizontal stainless steel tubes with the inner diameter of 0.3 mm and 1.5 mm. The testing conditions were performed with the mass fluxes range from 200 to 500 kg/m²s, the heat fluxes from 10 to 20 kW/m², the saturation temperature of 10°C and the vapor quality from 0.1 to dry-out. The effects of mass flux and heat flux on the heat transfer coefficient and pressure drop were analyzed. The experimental data were also compared with some well-known heat transfer coefficient and pressure drop correlations. A modified heat transfer coefficient correlation for alternative and natural refrigerants was proposed and predicted well the present experimental data

1. INTRODUCTION

In recent decades, natural refrigerant such as propane (R290), ammonia (NH₃), carbon dioxide (CO₂) and low global warming potential refrigerant such as R32, R1234yf are expected to be the promising candidates for the next refrigerant generation. However, both R290 and R32 have not been used commonly in refrigeration system due to their flammability. The solution may come up by using the mixture composed of R32 and R290 that can decrease the hydrocarbon flammability (Higashi, 2004). One of the other solution is to reduce the refrigerant charged by using the heat exchanger with small hydraulic diameter tube or parallel channels.

In the open literature, various papers demonstrate the boiling heat transfer performance of R32 and R290 in macro channel, which have the inner diameter larger than 3 mm (Shin et al., 1997; Choi et al., 2000; Wu et al., 2012; Hossain et al., 2013) but there are limited papers concerned with small tube (Fernando et al., 2008a, Choi et al., 2009). Hence the aim of this study is to investigate the boiling heat transfer coefficient of R290 and R32 in micro- and mini-channel with the hydraulic diameter of 0.3 mm and 1.5 mm. The effect of mass flux and heat flux on heat transfer coefficient and pressure drop of each refrigerant were well demonstrated. The experimental data was also compared with numerous existing heat transfer coefficient and pressure drop correlations.

2. EXPERIMENTAL APPARATUS

2.1 Experimental facilities

The experimental apparatus is comprised of the refrigerant loop, three auxiliary loops, and the data acquisition system. The schematic diagram of the refrigerant loop is shown in Figure 1. The refrigerant flow system consists of a condensing unit, receiver, magnetic gear pump, mass flow meter, and preheater. Vapor phase refrigerant from the evaporative test section was condensed into the liquid phase in the condensing unit. The condensed refrigerant was then accumulated in the receiver. The gear pump will deliver the liquid into the test section. The flow rate of the refrigerant was varied by controlling the pump speed via a motor controller and measured by a Coriolis-type mass

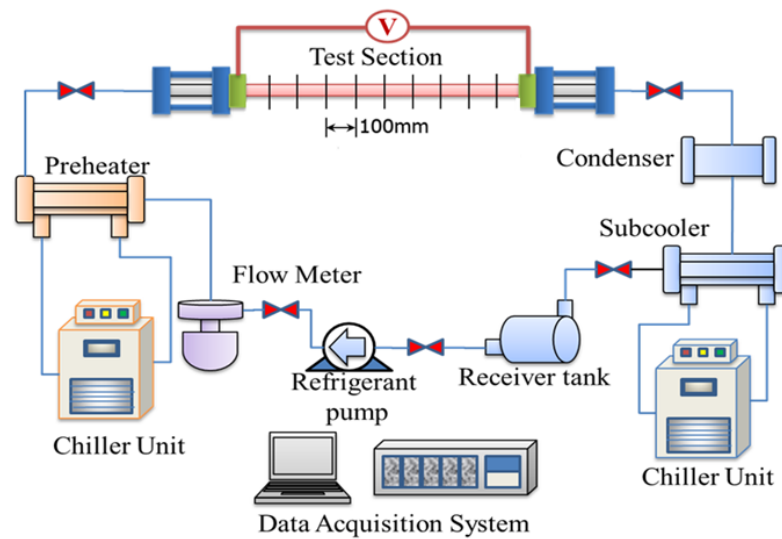


Figure 1: The experimental apparatus

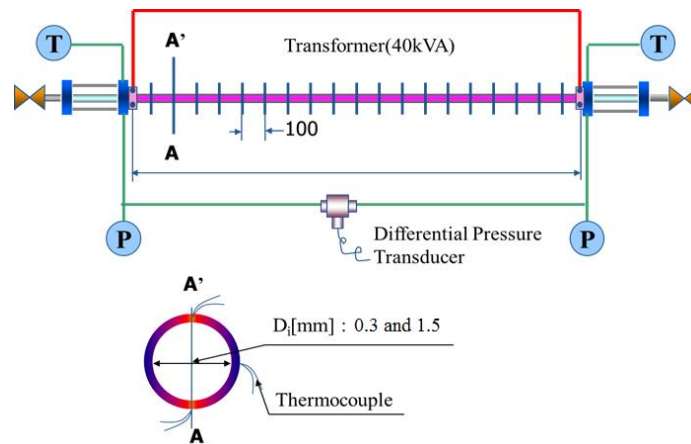


Figure 2: Schematic of test sections

flow meter. The mass quality at the inlet of the test section was controlled using a preheater. Temperatures of condenser, sub-cooler and preheater were adjusted by three individual water loops.

The test sections were made of circular stainless steel smooth tubes with inner diameter of 0.3 and 1.5 mm respectively. For evaporation at the test section, power was conducted from an electric transformer to the test section. The input electric voltage and current were adjusted to control the heat flux. The test section was well insulated with rubber and foam. The outside tube wall temperatures at the top, middle and bottom side were measured at every 100 mm axial intervals of the heated length using thermocouples at each measured site. The local saturation pressure, which was used to determine the saturation temperature, was measured using Bourdon tube-type pressure gauges at the inlet and the outlet of the test section. The pressure transducer was also installed to measure the pressure gradient of the refrigerant flowing along from the inlet to the outlet of the test section. Sight glasses with the same inner diameter as the test section and the length of 200 mm, were installed to visualize the flow and to enhance the flow stability of the fluid before entering the test section. The detail of test section was shown in Figure 2.

2.2 Data reduction

Table 1: The expanded uncertainty

Parameter	Uncertainty
T type thermo.	0 °C at 100 °C
Absolute pressure	±0.2 %
Different pressure	±2.5 kPa
G refrigerant	±0.2 %
G water	±0.2 %

2.2.1 Heat transfer coefficient data reduction

The measured saturation pressure at the inlet and outlet of the test section was used to obtain the local physical properties of the refrigerant. The mass quality x along the test section was determined based on the local thermodynamic properties:

$$x = \frac{i - i_f}{i_{fg}} \quad (1)$$

Where i is the enthalpy [kJ kg⁻¹], f is the saturated liquid condition, and g is the saturated vapor condition. The local heat transfer coefficient h along the length of the test section is defined as follows:

$$h = \frac{q}{T_{wi} - T_{sat}} \quad (2)$$

Where q is the heat flux [kW/m²], T is the temperature [K], w is a tube wall of the test section, i is the inner side, and sat is the saturation condition. The inside tube wall temperature T_{wi} is the average temperature of the top and bottom wall temperatures, and is determined using steady-state one-dimensional radial conduction heat transfer through the test section wall. The saturation temperature T_{sat} was obtained from the measured saturation pressure P_{sat} .

2.2.2 Frictional Pressure drop data reduction

The total pressure drop of two phase fluid is general calculated by sum of the static head Δp_{static} , the momentum $\Delta p_{momentum}$ and the frictional pressure drop $\Delta p_{frictional}$

$$\Delta p_{total} = \Delta p_{static} + \Delta p_{mom} + \Delta p_{frict} \quad (3)$$

Since the horizontal tube was used in this study, the pressure head can be neglected. The refrigerant is evaporated from liquid at the saturation temperature to vapour-liquid mixture at mass quality x with a linear change of test distance over the tube length. Hence the momentum pressure drop can be calculated following equation

$$-\left(\frac{dp}{dz}a\right) = G^2 v_f \left[\frac{x^2}{\alpha} \left(\frac{v_g}{v_f} \right) + \frac{(1-x)^2}{1-\alpha} - 1 \right] \quad (4)$$

For horizontal tube, void fraction α is defined by Steiner (1993) equation that was modified from Rouhani-Axelsson model.

$$\alpha = \frac{x}{\rho_g} \left[(1 + 0.12(1-x)) \left(\frac{x}{\rho_g} + \frac{1-x}{\rho_f} \right) + \frac{1.18(1-x) [g \sigma (\rho_f - \rho_g)]^{0.25}}{G \rho_f^{0.5}} \right]^{-1} \quad (5)$$

2.2.3 Uncertainty

According to the ISO guide to the expression of uncertainty in measurement (1995), the estimated ones in this study were obtained that included both the repeated observation and the calibration uncertainties. The calibration uncertainties were performed from the manufactory industry and shown in table 1.

The uncertainties of measurement data were calculated to be the mean of standard deviation. The uncertainty of heat transfer coefficient was evaluated by the least square method of combining the uncertainties of measurable quantities (temperature, heat flux and pressure). This study reported the uncertainty at 95% of confident level. For each test, 300 data points were collected in 5 minutes. Hence, the coverage factor k was approximate 2. The experimental of uncertainties of heat transfer coefficient, heat flux, pressure drop and temperature were $\pm 10\%$, $\pm 3\%$, $\pm 1\%$ and $\pm 0.35\text{ }^{\circ}\text{C}$, respectively.

3. RESULTS AND DISCUSSIONS

3.1 Heat transfer coefficient

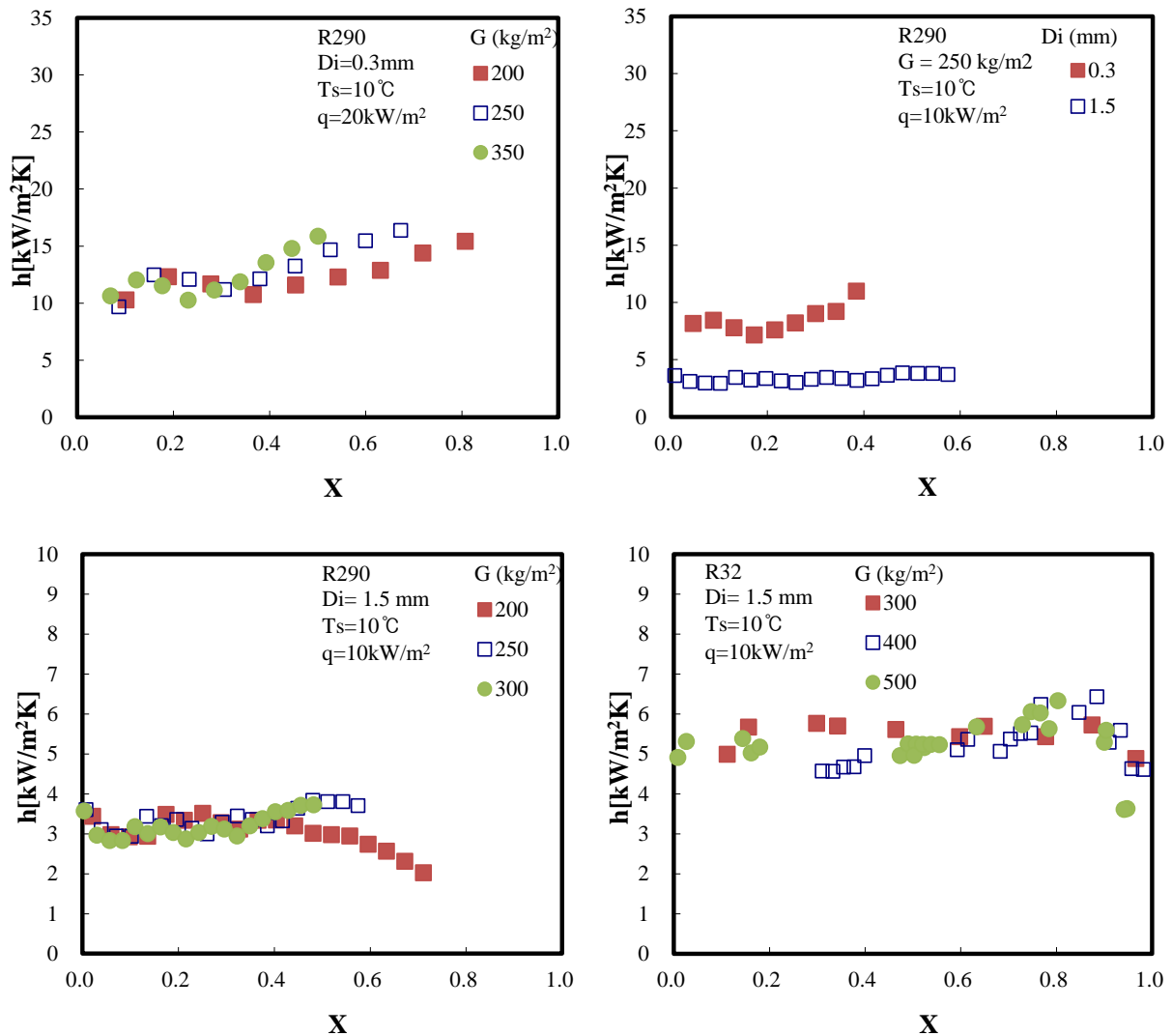


Figure 3: The effect of mass flux and tube diameter on heat transfer coefficient

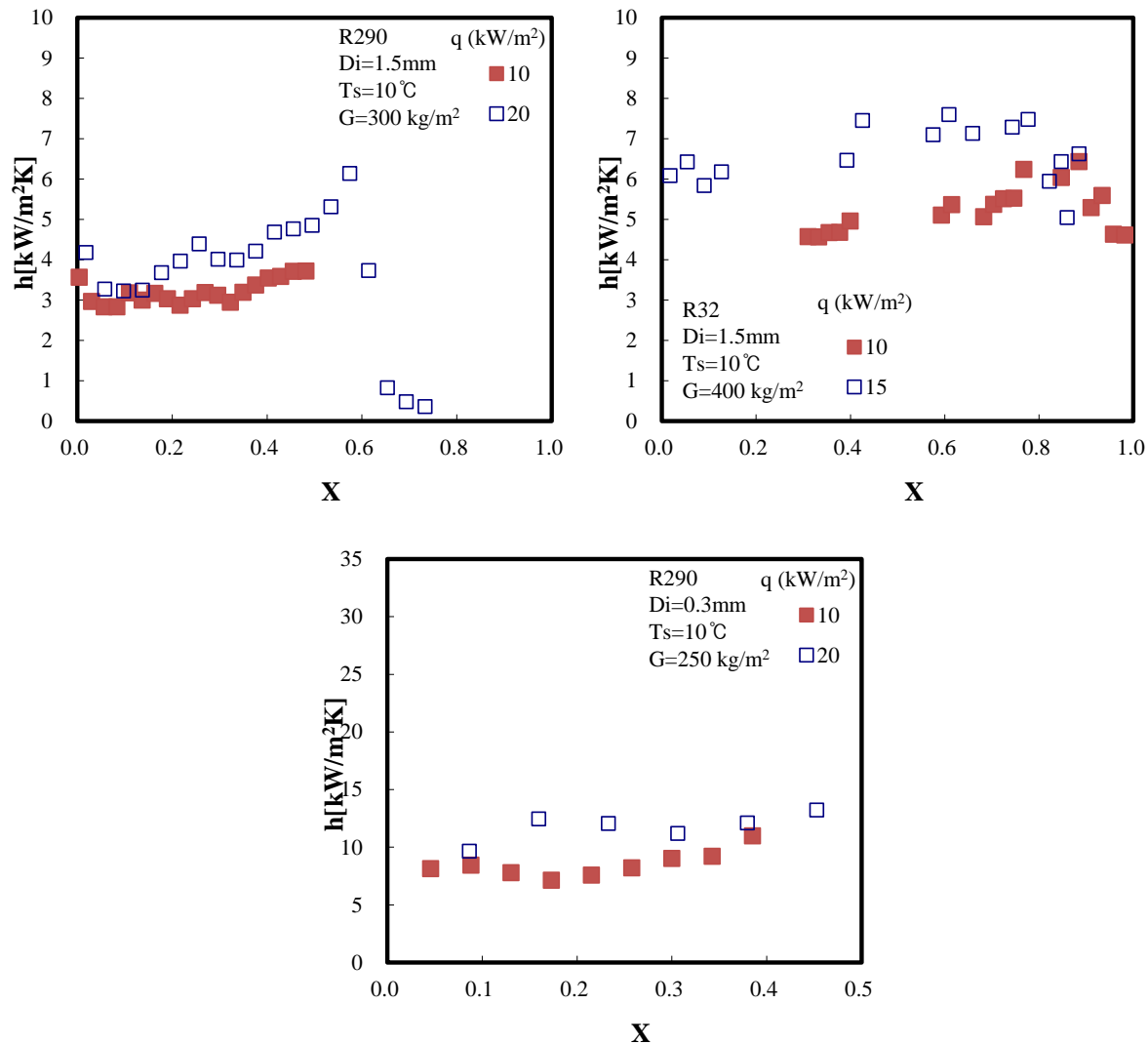


Figure 4: The effect of heat flux on heat transfer coefficient

Figure 3 illustrates the effect of mass flux on the heat transfer coefficient. The applied heat flux was fixed at 10 kW/m² and 20 kW/m² while the mass flux was ranged from 200 to 500 kg/m²s. The trends show that the mass flux has small effect on the heat transfer coefficient of R290 in low quality regime ($x < 0.4$). At higher one ($x > 0.4$), the higher mass flux conditions raise the higher heat transfer coefficient. For the cases of R32, the mass flux show an insignificant effect on whole regime. Moreover, as seen in the figure, heat transfer coefficient of R290 in 0.3 mm inner diameter tube is higher than that one in 1.5 mm inner tube.

The effect of heat flux on heat transfer coefficient of R32 and R290 was depicted in Figure 4. The graphs show the strong effect of mass flux on heat transfer coefficient. The heat transfer coefficient is higher with the higher heat flux. The contribution of nucleate boiling is dominant in present experimental data. On the other hand, the trends show that the dry out of R290 and R32 occurred at moderate quality regime of 0.6 and 0.8, respectively. It can be explained by considering the physical properties of refrigerants. At the same saturation temperature, the dry out normally occur later with the one that has higher surface tension.

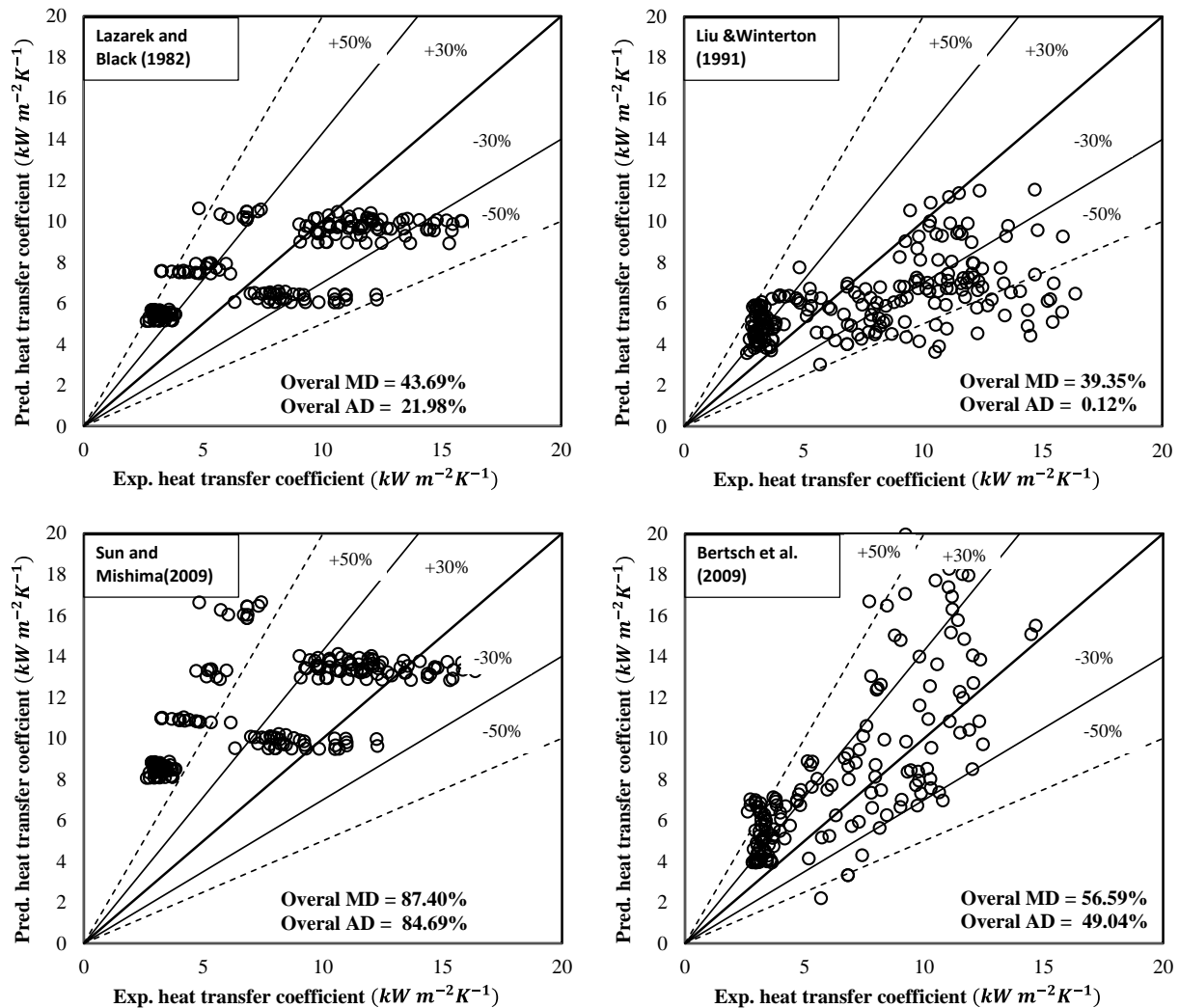


Figure 5: Comparison of experimental heat transfer coefficient with some heat transfer coefficient correlations

The comparison of experimental heat transfer coefficient with some well-known correlation is depicted in Figure 5. Four heat transfer coefficient correlations proposed by Lazarek and Black (1982), Liu and Winterton (1991), Beartsch et al. (2009) and Sun and Mishima (2009) were used in comparison. Among them, the one developed by Liu and Winterton (1991) shows the best prediction with the mean deviation of about 40%.

3.2 Development of heat transfer coefficient correlation

In the open literature, numerous studies such as J.R.Thome (2004), Cheng and Mewes (2006) showed that the heat transfer coefficient correlation for conventional tube could not predict well the heat transfer coefficient of minichannel. In addition, Bertsch et al. (2009) reviewed several heat transfer correlations for both minichannels and microchannels. The study noted that most of them developed based on small testing conditions and consequently, these correlations did not extrapolate well beyond their often narrow operating range. Therefore, in the present work the modified heat transfer coefficient correlations were developed using our data. The formula was based on the Chen correlation (1966) that used the physical superposition approach.

The flow boiling heat transfer in a tube, following Chen correlation (1966), mainly consist two mechanisms: nucleate boiling and forced convective evaporation. A superposition model of the heat transfer coefficient may be written as follows:

$$h_{tp} = Fh_{lo} + Sh_{pb} \quad (6)$$

The factor F is introduced as a convective two-phase multiplier to account for enhanced convection due to co-current flow of liquid and vapor by Chen, where $F = fn(X_{tt})$. Since the effect of small tube that make the convective heat transfer for evaporating refrigerant in small tube delayed with that in conventional tubes, the function should be physically evaluated again. Zhang et al. (2004) introduced a relationship between the factor F and the two-phase frictional multiplier that is based on the pressure gradient for liquid alone flow, $F = f(\phi_f^2)$ Where

$$\phi_f^2 = 1 + \frac{C}{X} + \frac{1}{X^2} \quad (7)$$

For liquid–vapor flow conditions of turbulent–turbulent (tt), laminar–turbulent (vt), turbulent–laminar (tv), and laminar–laminar (vv), the values of the Chisholm (1967) parameter C are 20, 12, 10, and 5, respectively. The Martinelli parameter, X, is defined as follows:

$$X = \left[\left(-\frac{dp}{dz} F \right)_f / \left(-\frac{dp}{dz} F \right)_g \right]^{1/2} = \left(\frac{f_f}{f_g} \right)^{1/2} \left(\frac{1-x}{x} \right) \left(\frac{\rho_g}{\rho_f} \right)^{1/2} \quad (8)$$

Where $(dp/dz F)$ is the pressure gradient due to friction (kPa/m) and ρ is the density (kg m⁻³). The friction factor f in Eq. (8) was obtained by considering the flow conditions of laminar - turbulent flows where $f=16Re^{-1}$ for $Re < 2300$ (laminar flow) and $f=0.079Re^{-0.25}$ for $Re > 3000$ (turbulent flow). The liquid heat transfer coefficient is defined by the Dittus – Boelter correlation (1930):

$$h_{lo} = 0.023 \frac{k_f}{D} \left[\frac{G(1-x)D}{\mu_f} \right]^{0.8} \left(\frac{c_{pf}\mu_f}{k_f} \right)^{0.4} \quad (9)$$

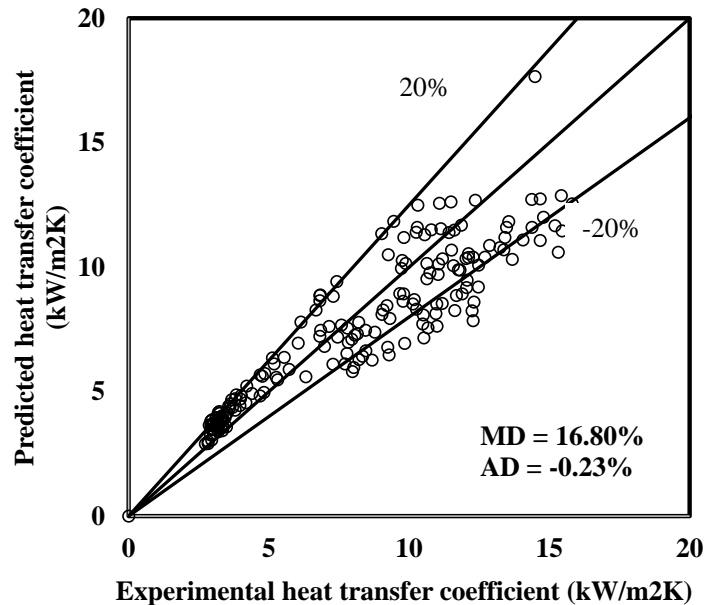


Figure 6: Comparison of experimental heat transfer coefficient with proposed heat transfer coefficient correlations

The F factor proposed by Zhang (2004) did not cover all the operating conditions in this work. Hence, a new factor F was developed from our experimental data using regression method. Note that, the minimum value of enhancement factor equals to 1 for pure liquid or pure vapor. Hence, its formula was proposed as:

$$F = \text{MAX} \left[a_1 (\phi_f)^{b_1} + c_1, 1 \right] \quad (10)$$

Using the regression program, the values of factor $a_1; b_1; c_1$ were determined as 0.006, 2 and 1.15, respectively.

The nucleate boiling heat transfer of the experimental data was predicted using the Cooper correlation (1984). For a surface roughness of $1.0\mu\text{m}$, the correlation is given as follows:

$$h_{pb} = 55 P_r^{0.12} (-0.4343 \ln P_r)^{-0.55} M^{-0.5} q^{0.67} \quad (11)$$

The nucleate boiling suppression factor S in our correlation is function of boiling number Bo and two-phase frictional multiplier. Using the experimental data from this study, a new nucleate boiling suppression factor, a ratio of h_{nbc} / h_{pb} , is proposed as follows

$$S = a_2 (\phi_f^2)^{b_2} Bo^{c_2} \quad (12)$$

Where a_2, b_2 and c_2 were evaluated as 0.13, 0.12 and -0.235, respectively. The comparison of heat transfer coefficient between the experimental data and prediction using our correlation is shown in Figure 6. The proposed correlation shows a good prediction with the mean deviation of 20.23 %

3.2 Pressure drop

The effect of mass flux and heat flux on pressure drop of R290 and R410A are described in Figure 7. The results shows the strongly influence of pressure drop on the mass flux and heat flux. The pressure drop both increases with the increasing of mass flux and heat flux.

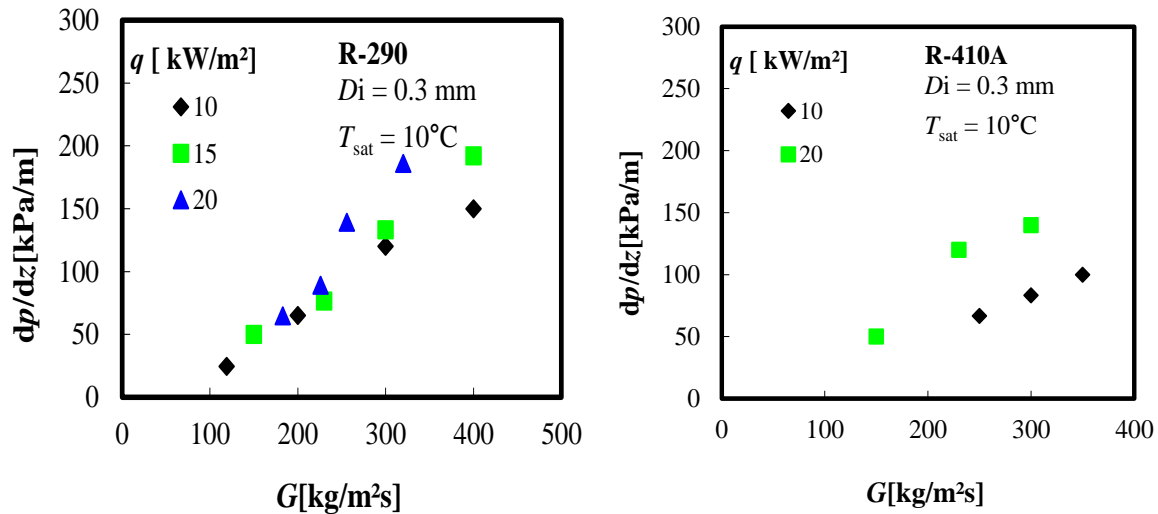


Figure 7: The effect of mass flux and heat flux on pressure drop

6. CONCLUSIONS

The experimental heat transfer coefficient and pressure drop of R410A, R32 and R290 were demonstrated in this study. Through the experimental results, the main finding can be summarized as following:

- The experimental results showed that the heat transfer coefficient of R32 and R290 increased with the increasing of heat flux. The contribution of nucleate boiling is dominant.
- The frictional pressure gradient is higher with the higher mass flux and heat flux.
- The present data was compared with various heat transfer coefficient correlations developed for minichannel. Among them, the one proposed by Liu and Winterton (1991) shows the best prediction. In addition, a modified heat transfer coefficient correlation was also developed using present data. The mean and average deviations were reported about 16.80% and -0.23 %, respectively.

REFERENCES

- Anowar Hossain, M., Onaka, Y., Afroz, H. M. M., & Miyara, A. (2013). Heat transfer during evaporation of R1234ze(E), R32, R410A and a mixture of R1234ze(E) and R32 inside a horizontal smooth tube. *International Journal of Refrigeration*, 36(2), 465–477.
- Bertsch, S. S., Groll, E. a., & Garimella, S. V. (2009). A composite heat transfer correlation for saturated flow boiling in small channels. *International Journal of Heat and Mass Transfer*, 52(7-8), 2110–2118.
- Chisholm, D. 1967, A theoretical basis for the Lockhart–Martinelli correlation for two-phase flow. *Int. Journal of Heat Mass Transfer* Vol. 10, 1767–1778.
- Chen, J. C., 1966, “A correlation for boiling heat transfer to saturated fluids in convective flow”, *Industrial and Engineering Chemistry, Process Design and Development* 5, 322-329 (1966).
- Choi, K.-I., Pamitran, a. S., Oh, J.-T., & Saito, K. (2009). Pressure drop and heat transfer during two-phase flow vaporization of propane in horizontal smooth minichannels. *International Journal of Refrigeration*, 32(5), 837–845.
- Choi, T. Y., Kim, Y. J., Kim, M. S., & Ro, S. T. (2000). Evaporation heat transfer of R-32, R-134a, R-32/134a, and R-32/125/134a inside a horizontal smooth tube. *International Journal of Heat and Mass Transfer*, 43, 3651–3660.
- Cooper, M.G., 1984. Heat flow rates in saturated nucleate pool boiling—a wide-ranging examination using reduced properties. *Advances in Heat Transfer* 16, 157 – 239 (Academic Press).
- Fernando, P., Palm, B., Ameel, T., Lundqvist, P., & Granryd, E. (2008a). A minichannel aluminium tube heat exchanger – Part II: Evaporator performance with propane. *International Journal of Refrigeration*, 31(4), 681–695.
- Higashi, Y. (2004). Experimental determination of the critical locus for the difluoromethane (R32) and propane (R290) system. *Fluid Phase Equilibria*, 219(1), 99–103.
- L. Cheng and D. Mewes. Review of two-phase flow and flow boiling of mixture in small and mini channels. *International Journal of Multiphase Flow*. Vol 32, no. 2, pp. 183-207, 2006.
- Lazarek, G., & Black, S. (1982). Evaporative heat transfer, pressure drop and critical heat flux in a small vertical tube with R-113. *International Journal of Heat and Mass Transfer*, 25(7).
- Liu, Z., & Winterton, R. (1991). A general correlation for saturated and subcooled flow boiling in tubes and annuli, based on a nucleate pool boiling equation. *International Journal of Heat and Mass Transfer*, 34(11), 2759–2766.
- Shin, J. Y., Kim, M. S., & Ro, S. T. (1997). Experimental study on forced convective boiling heat transfer of pure refrigerants and refrigerant mixtures in a horizontal tube. *International Journal of Refrigeration*, 20(4), 267–275.
- Steiner, D., 1993. VDI-Warmeatlas (VDI Heat Atlas) chapter Hbb. In: Verein Deutscher Ingenieure, editor. VDI-€Gesellschaft Verfahrenstechnik und Chemieingenieurwesen (GCF), Translator: J.W. Fullarton, Dusseldorf.
- Sun, L., & Mishima, K. (2009). An evaluation of prediction methods for saturated flow boiling heat transfer in mini-channels. *International Journal of Heat and Mass Transfer*, 52(23-24), 5323–5329.
- Wu, J. H., Yang, L. D., & Hou, J. (2012). Experimental performance study of a small wall room air conditioner retrofitted with R290 and R1270. *International Journal of Refrigeration*, 35(7), 1860–1868.
- Zhang, W., Hibiki, T. and Mishima, K., 2004. Correlation for flow boiling heat transfer in mini-channels. *Int. J. Heat Mass Transfer* 47, 5749–5763.

NOMENCLATURE

AD	Average Deviation,	c_p	Specific heat	(kJ kg ⁻¹ K ⁻¹)
----	--------------------	-------	---------------	--

B_o	Boiling number		C	Chisholm parameter
D	Diameter	(m)	f	Friction factor
G	Mass flux	(kg m ⁻² s ⁻¹)		
g	Acceleration due to gravity	(m s ⁻²)		
L	Tube length	(m)	MD	Mean Deviation,
h	heat transfer coefficient	(kW m ⁻² K ⁻¹)	$MD = \left(\frac{1}{n} \right) \sum_{i=1}^n \left \left(dp_{pred} - dp_{exp} \right) \times 100 / dp_{exp} \right $	
I	enthalpy	(kg kJ ⁻¹)		
P	Pressure	(kPa)		
q	Heat flux	(kW m ⁻²)	Re	Reynolds number, $Re = GD/\mu$
T	Temperature (K)			
X	Lockhart-Martinelli parameter			
x	Vapor quality	(-)		
z	Length	(m)		
Greek letters				
α	Void fraction		μ	Viscosity (Pa·s)
ρ	Density (kg m ⁻³)		σ	Surface tension (N m ⁻¹)
ϕ^2	Two-phase frictional multiplier		(dp/dz)	Pressure gradient (N m ⁻² m ⁻¹)
(dp/dz F)	Pressure gradient due to friction (N m ⁻² m ⁻¹)			
Subscripts				
crit	Critical point		exp	Experimental value
f	Saturated liquid		g	Saturated vapor
fric	Frictional		mom	Momentum
i	Inner tube		lo	Liquid only
o	Outer tube		pb	Pool boiling
pred	Predicted value		r	Reduced
sat	Saturation		sc	Subcooled
t	Turbulent		tp	Two-phase
v	Laminar		w	Wall
n	Number of data			

ACKNOWLEDGEMENT

This research was supported by Basic Science Research Program through the National Research Foundation of Korea (NRF) funded by Ministry of Education, Science and Technology (NRF-2013R1A1A2013476)